IOP Publishing Phys. Med. Biol. 67 (2022) 125011 https://doi.org/10.1088/1361-6560/ac6ebb

Physics in Medicine & Biology

IPEM Institute of Physics and Engineering in Medicine

PAPER

The influence of hypoxia on LET and RBE relationships with implications for ultra-high dose rates and FLASH modelling

Bleddyn Jones

Gray Laboratory, University of Oxford Department of Oncology, Old Road Campus Research Building, Oxford OX3 7DQ, United Kingdom

E-mail: Bleddyn.Jones @oncology.ox.ac.uk

Keywords: radiotherapy, flash, rbe, oxygen effect, protons, ions

OPEN ACCESS

RECEIVED
2 November 2021

REVISED
22 April 2022

ACCEPTED FOR PUBLICATION
11 May 2022

PUBLISHED
10 June 2022

Abstract

Objective. To investigate relationships between linear energy transfer (LET), fluence rates, changes in radiosensitivity and the oxygen enhancement ratio (OER) in different ion beams and extend these concepts to ultra-high dose rate (UHDR) or FLASH effects. *Approach.* LET values providing maximum relative biological effect (RBE), designated as LET_U, are found for neon, carbon and helium beams. Proton experiments show reduced RBEs with depth in scattered (divergent) beams, but not with scanned beams, suggesting that instantaneous fluence rates (related to track separation distances) can modify RBE, all other RBE-determining factors being equal. Micro-volumetric energy transfer per μm^3 (mVET) is defined by LET $\times$ fluence. High fluence rates will increase mVET rates, with proportional shifts of LET_U to lower values due to more rapid energy transfer. From the relationship between LET_U and OER at conventional dose rates, OER reductions in UHDR/FLASH exposures can be estimated and biological effective dose analysis of experimental lung and skin reactions becomes feasible. *Main results.* The Furusawa *et al* data show that hypoxic LET_U values exceed their oxic counterparts. OER reduces from around 3–1.25 at LET_U, although the relative radiosensitivities of the oxic and hypoxic α parameters (the $OER_{(\alpha)}$) exceed those of the standard OER values. Increased fluence rates are predicted to reduce LET_U and OER. Large FLASH single doses will minimise RBE increments due to the β parameter reducing by a factor of 0.5–0.25 consistent with oxygen depletion, causing radioresistance. Similar results will occur for photons. Tissue α/β ratios increase by around 10 in FLASH conditions, agreeing with derived ion-beam dose rate equations. *Significance.* Increasing dose rates enhance local energy deposition rate per unit volume, probably causing oxygen depletion and radioresistance in pre-existing hypoxic sites during UHDR/FLASH exposures. The modelled equations provide testable hypotheses for further dose rate investigations in photon, proton and ion beams.

Introduction

To study the likely sequential mechanisms of why ultra-high dose rates and FLASH radiotherapy induce acquired radioresistance requires integration of knowledge across many areas of radiobiology and fundamental dosimetry. The concepts of fluence, linear energy transfer (LET), relative biological effectiveness (RBE) which increases radiosensitivity with LET, oxygen enhancement ratio (OER) which reduces radiosensitivity with diminishing oxygen levels, and the biological effective dose (BED) concept based on the linear quadratic (LQ) model of radiation effect, must all be thoroughly understood. The subtle impact on radiochemistry of fluence rate in comparison with total fluence must also be appreciated, along with basic micro-dosimetry concepts such as the distinction between LET along individual radiation tracks, and the product of fluence$\times$LET being the volumetric energy transfer especially within small cubic-micrometre volumes of interest.

Energetic charged particles have a LET-RBE relationship which increases with LET until a maximum or peak RBE (and radiosensitivity) is obtained at a LET value of LET_U, which is unique (rather than a common shared value) for each ion species, and generally increases with Z. The probability of this being a random effect is

1/7! = 0.0002, for seven ions (H, He, C, Ne, A, Si and Fe) studied previously (Jones and Hill 2019). Beyond LET_U the RBE falls with higher LET due to overkill effects. Studies of charged particle kinematics and particle ranges at conventional dose rates have suggested that various ions with different Z values share common features in terms of their charge per unit velocity and mass at LET_U, although residual particle ranges increase considerably with Z (Jones and Hill 2019, 2020). Z-specific LET_U values can be used to scale estimates of increasing radiosensitivities (and associated RBE) with increasing LET for any ion species (Jones 2015). These experimental irradiations used conventional dose rates (typically 0.5–15 Gy per minute), so it is possible that these relationships may change at higher dose rates.

Some experimental data sets have also studied oxygenation effects on RBE and radiosensitivities over a range of LET values below and above LET_U (Barendsen *et al* 1966, Furusawa *et al* 2000, Furusawa *et al* 2012). These data show that the OER values (determined by the larger dose in hypoxia divided by the lower dose in oxic conditions) required to achieve the same biological effect, are progressively reduced with increasing LET, falling from around 3 to 1.25 at the LET_U RBE turnover point and continue to decrease with further LET increases to be close to unity. Formal definitions of RBE and OER and examples of their relative magnitudes are given in appendix A with some comments on oxygen depletion during radiation exposure. These must be fully understood before proceeding further.

Such difficult and costly experiments were designed to demonstrate the overall phenomena, many having small numbers of data points for statistical analysis, with no uncertainties provided. However, these experiments remain the best available and continue to provide an important data source, and can be used to develop hypotheses and models based on point estimates sufficient for tentative modelling purposes.

The present study investigates these phenomena, especially changes in the α and β radiosensitivity parameters with LET in hypoxic and oxic states, and the changes in LET_U values with increasing dose rates. Data from using Neon and Carbon ions are used to predict the responses found with helium ions. It is then possible to speculate what might occur with protons, as well as when instantaneous fluence, or dose rates become very large for any form of radiation.

There is experimental evidence that RBE can be influenced by the instantaneous fluence rate, which is itself related to mean particle inter-track distances (Calugaru *et al* 2011, Britten *et al* 2013, Jones *et al* 2018). Increasing fluence rates and reduction of inter-track distances will inevitably allow a more rapid increase of total energy transfer (rather than in LET *al*ong each track) within critical 1 μm^3 volumes, which are relevant to chromosomal thickness and lethal chromosome breakage. There will also be consequent effects on the OER due to more rapid localised oxygen depletion caused by ionisation and hydrolysis around tracks.

LET is itself an averaged value, with considerable variation along tracks. But in some locations, there will be far more clustered ionisation capable of causing cell death. The frequency of such clusters will correlate with the average value.

By studying each sequential mechanism, the present study investigates how increasing dose rates can influence the OER and radiosensitivity. These are:

1. Higher fluence rates will increase the energy transfer rate per unit micro-volume (1 μm^3), since fluence rate (per $\mu m^2.sec^{-1}$)$\times$ LET $=$ Energy transfer per 1 μm^3 volume per second.
2. Increased fluence rates and energy transfer rates should have the same effect as high LET radiations towards their turnover point for RBE effects (at LET_U), despite the actual LET being unchanged (only the fluence rate has changed).
3. At LET_U, multiple ion beam data show reductions in OER from 3 to around 1.25.
4. More rapid energy transfer rates (per 1 μm^3 volume per second) provide a total energy transfer similar to at LET_U(when using standard dose rates for ions), which should cause faster oxygen depletion, reducing the OER (as found with high LET radiations). This should occur regardless of the radiation modality used.
5. The resulting reduced OER is radio-protective. This will occur in situations where there is transient hypoxia, including normal tissues where phasic blood flow conditions exist, since only a relatively small change in oxygen tension is necessary to cause significant radioresistance.
6. The same dose rate effects should occur when using low LET radiations (photons and electrons) at sufficiently high dose rates, or with positive charged particle beams at much lower LET values than their standard dose rate LET_U values.
7. The LQ model α and β radiosensitivity parameters normally reduce in hypoxia at conventional dose rates. With high single doses, β parameter effects predominate over α effects in the LQ model. OER-related

reductions in β will cause substantial radioresistance, and overcome any limited increase in β due to closer ionisations.

8. The entire process can in principle be modelled in terms of the BED concept, based entirely on the LQ model of radiation effect.

These mechanistic steps and data analysis are presented in greater detail below.

Methods and descriptions of models

The ion beam data sets of Furusawa *et al* (2000), Furusawa *et al* (2012) (neon, carbon and helium ions accelerated in cyclotrons), Barendsen *et al* (helium ions and deuterons accelerated with a cyclotron) (Barendsen *et al* 1966), and Weyrather *et al* (carbon ions accelerated by a synchrotron) (Weyrather *et al* 1999) are used. The helium data included publications of RBE and OER values with LET, although no α radiosensitivity values were provided. Furusawa *et al* (2000), Furusawa *et al* (2012) provided α radiosensitivity values only in tabular form, without standard errors. For this reason, graphical data presentations are used, with least squares fitting (using *Mathematica*, Wolfram software) of the lines and curves leading to and beyond the apparent turnover points in oxic and hypoxic conditions respectively in order to estimate LET_U for each condition.

By finding the LET_U values in oxic and hypoxic conditions for ions of different Z values, it is possible to speculatively extrapolate to protons. Proton LET_U values are controversial and estimates range from around 30 keV.μm^{-1} (a value restricted by experimental mono-energetic proton beam ranges at lower energies) to around 60 keV.μm^{-1} in a fast-neutron beam which produces recoil protons fairly uniformly with depth, without the severe particle range limitations which restrict experimental mono-energetic proton experiments (Jones 2021). LET values of 60 keV.μm^{-1} and above will occur in high energy proton beams but only over small distances toward the very end of range (Jones and Hill 2020).

Proton beam evidence for the effect of fluence rate on RBE

Analysis of experimental data has shown that divergence geometry can influence proton RBE. In the case of passively scattered beams, RBE falls from over 1.3 to around 1.03 with increasing depth (Calugaru *et al* 2011) in two cell lines, but with scanned beams no such fall occurs (Britten *et al* 2013). The LET distributions, total fluences, and dose were the same at the two extremes of depth used in both studies, but the only striking difference to explain these significant RBE effects was that the treatment time was significantly longer at the greatest depths in scattered beams because of inverse-square law effects reducing their fluence and dose rates.

The beam exposure times remained sufficiently short so that even the fastest DNA repair rates of 10–15 min could not account for the large RBE changes found. Consequently, it has been argued that the most likely explanation appears to be that instantaneous fluence is responsible (Jones *et al* 2018, Jones 2017, 2021), since this parameter changes markedly for divergent scattered beams with depth, but not for scanned beams until very close to their end of range. The total fluence is used to provide the intended dose per treatment by increasing the exposure time until the necessary (total) fluence is obtained. Importantly, the near instantaneous fluence is likely to govern the fundamental physico-chemical interactions (Wardman 2009) which commence within nanoseconds and the influence of oxygen is completed by a few tens of microseconds, as found in pulse radiolysis experiments (Watts *et al* 1978). Specially commissioned Geant 4 Monte Carlo (M-C) studies at Imperial College showed marked reductions in inter-track distances at short time intervals at the greatest depth only in scattered beams (David Collingwood, personal communication). Unpublished M-C studies of the entire treatment duration fail to show any differences at many research institutes, including FLUKA at Oxford, as would be expected.

Dose, fluence and time considerations

The relationship between dose (D) and fluence (F), the number of particle tracks per unit cross sectional area, in a medium of density ρ is

$$D = F(\mathrm{cm}^{-2}) \times LET \times 1.602 \times 10^{-9} \times \frac{1}{\rho}\,(\mathrm{cm}^3 g^{-1}). \quad (1)$$

Now D is the product of dose rate (R) and exposure time (T), so that the equation (1) containing fluence (F) can be simplified as

$$R.T = F.LET.K, \quad (2)$$

where K is a constant depending on the medium.

Equation (2) can be divided throughout by T, to give

$$R = \frac{F}{T}.LET.K, \tag{3}$$

which is further simplified by using F_R to represent the fluence rate, a.s.

$$R = F_R.LET.K. \tag{4}$$

Thus the dose rate R is associated with the fluence rate F_R independent of LET.

For two different dose rates (R_1 and R_2) which deliver the same dose D in times of T_1 and T_2 respectively, then

$$\frac{D}{T_1} = F_{R1}.LET.K \tag{5}$$

and

$$\frac{D}{T_2} = F_{R2}.LET.K. \tag{6}$$

Dividing equation (5) by equation (6) gives

$$\frac{T_2}{T_1} = \frac{F_{R1}}{F_{R2}}. \tag{7}$$

Thus the ratio of the treatment times is the same as the inverted ratio of the instantaneous fluence rates, provided that the same dose is given.

Over a short duration of time necessary to influence the radiolysis of water, the separation of particle tracks will be dependent on the fluence in that same time. To study averaged particle inter-track distances (S), it is standard to use $S = F^{-0.5}$ for cross sectional areas.

Average inter-track significant event distance (S')

It is necessary to consider not only inter-track distances but also the average distances (S') between randomly placed DNA damage events within the critical volume of interest, rather than per unit area, as used in the definition of fluence (number of beams per unit area). Such events are considered to be necessary precursors of lethal damage. Within any volume, it can be shown that S' is inversely proportional to the cube root of fluence, i.e. $\sqrt[3]{\frac{1}{F}}$. This is shown in appendix A.

The link between dose rates and fluence with increasing depth in divergent beams

As cross-sectional divergent beam areas increase with the square of distance or depth (d), so fluence will fall with increasing depth in a scattered beam, as will dose rate (R), which depends on the fluence per unit time.

The proportionality is expressed as

$$R = \frac{C}{d^2}. \tag{8}$$

where C is a constant.

For two different dose rates R_1 and R_2 at depth distances of d_1 and d_2 respectively, then

$$\frac{R_1}{R_2} = \frac{d_2^2}{d_1^2}. \tag{9}$$

Decreasing the fluence or dose rate will reduce the total energy deposition in very short times, with consequent increases in the mean inter-track distances within a volume of interest (e.g. 1 μm^3, which is relevant for a short section of a chromosome). This may reduce cooperative effects between tracks, but will also reduce the total energy deposition in a small volume in a small unit of time, and so potentially reduce the RBE.

For example, in the experiments of Calugaru *et al* (2011), a marked fall in RBE from just over 1.3 down to around 1.03 occurred between depth distances of 2 and 18 cm depth in their scattered beam.

The change in RBE above unity (from a value of RBE$_A$ at the initial depth d_A to become RBE$_B$ at depth d_B), when modified by fluence rate due to depth, can be expressed with inclusion of the inverse square law effect as:

$$RBE_B = 1 + (RBE_A - 1)\sqrt{\frac{d_A^2}{d_B^2}}, \tag{10}$$

where the square root function effectively considers the average inter-track distance *(S)* within a cross-section at a given depth, since $S = \sqrt{\frac{1}{F}}$ and S will increase with depth in a divergent beam. Any accompanying constants which link each of the distances to RBE will cancel in the ratio.

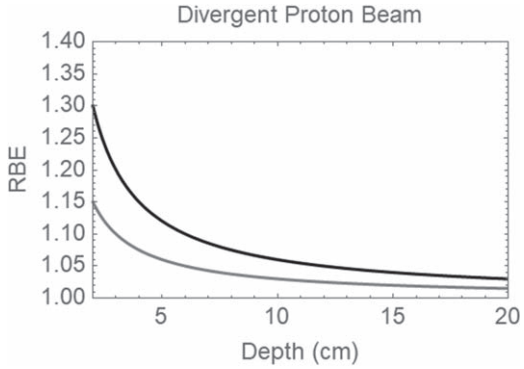

Figure 1. Plots of proton RBE with increasing depth obtained using equation (10), by varying the distance d_B, for assumed entrance RBE values of 1.15 and 1.3 at mid spread-out Bragg-peak (SOBP) (grey curve) and towards the end of SOBP (black curve) respectively. The SOBPs are assumed to be identical with respect to dose and LET distributions, but placed at different depths.

Thus an RBE of 1.3 at 2 cm would reduce to be:

$$RBE \text{ at } 18 \text{ cm} = 1 + (1.3 - 1)\sqrt{\frac{2^2}{18^2}} = 1 + 0.3 \times 0.9 = 1.033. \quad (11)$$

The theoretical relationship for intermediate distances is shown in figure 1.

This differs from a previous interpretation where an exponential function was assume to represent the fall off in RBE with depth (Jones 2017).

If RBE falls with increasing depth due to a reduction in instantaneous fluence rate (F_R) and associated larger inter-track distances (S), then it is reasonable to suggest that the converse will apply: namely that RBE will increase in situations when F_R increases and when S becomes much smaller. Reductions in S will enhance the initially small probability of cooperative effects between tracks within the time frame of the physico-chemical radiation changes, especially since individual charged particle tracks are associated with a surrounding 'cylinder' of secondary electrons as originally emphasised by Katz (Waligórski *et al* 2015). Such cooperative effects may or may not occur and need experimental verification and detailed computer simulations. However, the more rapid accumulation of energy per μm^3 may be a sufficient explanation for increased radiosensitivities and simultaneously reduced OERs, as considered next.

In order for radiosensitivities and RBE to increase with dose rate, the relationship between RBE and LET must change. When fluence rates increase, the product of LET and fluence rate (the volumetric LET or mVET per unit time) will increase, with treatment to the same dose being delivered in shorter times. Increasing energy transfer accumulation within micro-volumes will then increase radiosensitivity, just as found with increasing LET, where more clustered, unrepairable DNA damage, occurs. Such clustering increases radiosensitivity, achieved by mainly affecting the α parameter (Jones 2015). In other words, increasing fluence rate will cause increased radiosensitivity despite LET being unchanged, although mVET increases more rapidly until the entire mVET reaches the same total energy transfer which occurs at LET_U with conventional dose rates (and lower instantaneous fluences).

These volumetric principles are illustrated in figure 2 (panels a and b). The slope of the radiosensitivity α parameter (and RBE) with LET must increase at very high dose rates due to more rapid energy accumulation so that the apparent turnover LET_U will effectively occur at lower linear LET values than with conventional, lower fluence rates. These clustering and radiosensitivity changes will probably be accompanied *pari passu* by a reduction in the OER. Thus the OER reduction is itself expected to follow the enhancement of fluence rate and more rapid increases in local ionisation clustering with localised oxygen depletion. These effects and the changes in LET_U position will be shown in results below.

In equation (10), the distance-squared ratio term can be replaced by the dose rate ratio, or the instantaneous fluence-rate ratios, due to their proportionality.

Delivery methods for particle beams must next be considered. Cyclotrons generally deliver higher dose rates than synchrotrons. There may also be differences in dose rates between the reference radiations and particles in RBE estimations. Consequently, it is possible that variations of the LET_U values for specific ions may be due to differences in applied dose (or fluence) rates. For example, LET_U values of 202 and 177.8 keV.μm^{-1} are found for carbon ions in experiments at Darmstadt using a synchrotron (with lower dose rate) (Weyrather *et al* 1999), but lower LET_U estimates of 168.4 and 169.4 keV.μm^{-1} are obtained from experiments at NIRS (Chiba) in Japan where faster-operating cyclotrons were used (Jones and Hill 2019). Such limited evidence may be coincidental, but does not oppose the present hypothesis.

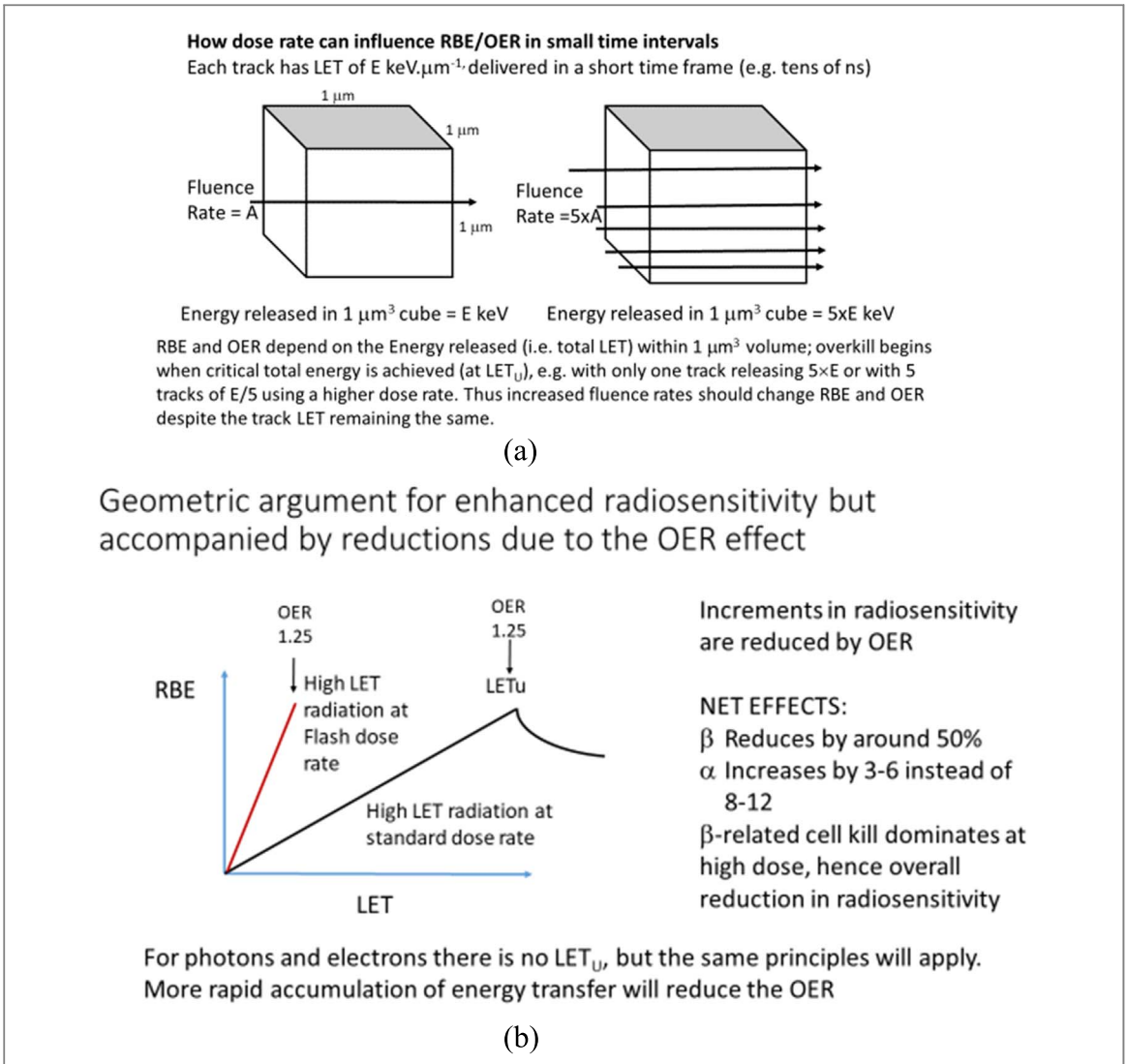

Figure 2. (panel (a)) Schematic diagram of energy deposition in say tens to hundreds of nanoseconds in a volume of 1 μm^3 and (b) effects on LET_U position and radiosensitivities by increasing the dose and fluence rate, which leads to a more efficient increase in RBE.

Incorporation of time changes to LET_U position

If LET_U reduces with increasing dose rate, there will also be OER consequences, since experiments have shown that the OER reduces in proportion to the increasing energy transfer in ion beams (Barendsen *et al* 1966, Furusawa *et al* 2000, Furusawa *et al* 2012). Where instantaneous fluence rates are high, mVET increases and the OER should then reduce more efficiently with increased LET. Also, as oxygen is depleted the hypoxic LET-RBE relationship will be followed (which increases the LET_U value at low dose rates), but will be overridden by a greater shift to lower values at very high fluence rates.

Estimates of such effects are made for a dose rate value LET_{U1} to become LET_{U2} at a higher dose rate, where fluence rates (here represented by exposure times) and their effects on average distance between damaged sites (S') within the volume of interest using the cubed root expression given above. Then, since S' is related to fluence rate, and so to time, then LET_U changes (relative to a reference LET of LET_{ref}) is expected to change in proportion to the cubed root of the exposure times T_1 and $T_2$for the standard dose rate and a faster dose rate respectively (where $T_2 < T_1$),:

$$LET_{u2} = (LET_{u1} - LET_{ref}).\sqrt[3]{\frac{T_2}{T_1}} + LET_{ref}. \quad (12)$$

Here time is used instead of dose rate when it is assumed that the same dose is delivered. This relationship is shown later in figure 7 of results below.

A similar function can be used for RBE (as in equation (10)), since there is direct proportionality between RBE and LET below LET_U (Jones 2015, Jones and Hill 2019, 2020) .

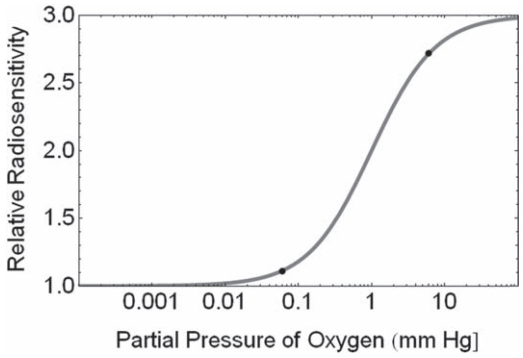

Figure 3. Relationship of partial pressure of oxygen and relative radiosensitivity (effectively the OER). The two points shown are for 3 mm Hg down and 0.05 mm Hg partial pressure, between which relative radiosensitivity changes by around 2.5 [Reproduced with permission from Wilson *et al* (2012), The British Institute of Radiology]. Ultra-high dose rate *in vitro* effects are most effective in conditions such as 3 mm Hg partial pressure, and were not be found in well oxygenated bio-systems.

The adjusted RBE (RBE_2) is then

$$RBE_2 = (RBE_1 - 1).\sqrt[3]{\frac{T_1}{T_2}} + 1, \tag{13}$$

where RBE_1 is the reference RBE estimate obtained with conventional dose rates and where the times are inverted compared with equation (12) for the increment, which is the excess RBE beyond a value of unity. The times used must only be those found in experiments where FLASH/UHDR effects have been found.

The same degree of OER reduction (to around 1.25 at LET_U) is assumed to occur at the modified LET_U position as for the unmodified LET_U, since the total energy transfer will be the same.

The parameter OER_α is defined as the ratio

$$OER_\alpha = \frac{\alpha_{oxic}}{\alpha_{hypoxic}}. \tag{14}$$

The comments on oxygen depletion by radiation made by Alper in appendix A should be noted again at this stage. This occurs due to rapid oxygen reactions with ionised water and oxygen fixation on damaged sites. Such oxygen depletion will occur around radiation tracks and damaged sites, and will be reversed by oxygen diffusion operating with a slower time course than that of the depletion process when dose rates are high. This is considered further below.

Experimental oxygen depletion is known to be non-linearly related to radiosensitivity over a wide range of oxygen partial pressure plotted on a log-scale abscissa (Wilson *et al* 2012), as shown in figure 3. Because of the shape of the relationship, the ultra-high dose rate effect will only change the cellular or tissue responses substantially when oxygen tension is already low and only a small change in Oxygen partial pressure, between 3 mm Hg and 0.1 mm Hg, is necessary. This necessity for existing hypoxia will also reduce the oxygen diffusion time since this will depend on the oxygen tension gradient. Estimations using standard diffusion equations show that between tensions of 3 mm Hg and 0.1 mm Hg, the diffusion times to distances of 0.5 and 1 μm respectively are around 30 and 140 msec, when most of the radiosensitivity change after short exposures is permanent (Watts *et al* 1978, Wardman 2009). Thus rapid radiation pulses in pre-existing hypoxic sites are more likely to deplete and maintain a state of oxygen depletion which can influence radiosensitivity.

Consequently, ultra-high dose-rate effect radiation-induced oxygen depletion will influence radiosensitivity significantly only in pre-existing hypoxic states, as concluded by Berry *et al* (Berry and Stedeford 1972).

The BED method

For comparisons between conventional dose rates and UHDR (or FLASH) dose rates on experimental murine lung fibrosis and skin reactions found by Vozenin *et al* (2019a, 2019b), the BED method can be used. BED is useful in many radiotherapy applications including low dose-rate effects. The equations contain biologically based α/β ratios, which are stable parameters in late reacting normal tissues (Jones and Dale 2018, Jones *et al* 2001), as in

$$BED = D\left(1 + \frac{D}{\alpha/\beta}\right), \tag{15}$$

for single doses of D Gy.

The lung fibrosis effect is published as categorical scores, which can be directly related to *BED* by assuming that a threshold dose (BED_0) has been exceeded. This is typically a *BED* of around 44.6–48.8 Gy, compatible with a single dose of around 11 Gy for α/β between 3.2 and 3.6 Gy (van Rongen *et al* 1993). It is necessary to assume a reasonable relationship between *BED* and the experimental grading category scores for both conventional and FLASH dose rates: a category (scores 1, 2 and 3) has an excess *BED* of 20, 40 and 60 Gy above the threshold value (effectively providing a dose response relationship of 13.4, 15.6 and 17.4 Gy single doses respectively for lung-reaction scores of 1, 2 and 3 for a typical α/β of 3.4 Gy) and so is compatible with published data. This excess *BED* is designated as BED^* (or $BED–BED_0$), where BED_0 is the threshold *BED* for the effect.

Least squares fits using Non-linear fitting techniques on Mathematica can be applied to the published data using the equation:

$$BED^* = d(1 + d/k) – C, \tag{16}$$

where d is the known dose (in single fractions here), k (the α/β ratio) and C (the intercept *BED* at zero dose) can then be estimated.

The threshold dose (d_S) for the effect will occur when $BED^* = 0$, when

$$d(1 + d/k) - C = 0, \tag{17}$$

C is then the BED threshold value. The dose under this condition will be the threshold dose, d_s, given by the solution of

$$d_s(1 + d_s/k) = C, \tag{18}$$

and where

$$d_s = (\sqrt{(1 + 4C)} - 1)/2. \tag{19}$$

Thus the data fitting provide estimates of α/β, C (the threshold *BED*) and d_S.

To convert from the standard (conventional dose-rate) α/β ratio to the FLASH α/β ratio, the exponent-modified ratio of treatment times, as in equations (12) and (13), is used as an operator (termed J), such that

$$J.(\alpha/\beta)_{conv} = (\alpha/\beta)_{flash}, \tag{20}$$

where conv and flash subscripts are used for conventional and FLASH parameters and exposure times, where

$$J = \left(\frac{T_{conv}}{T_{flash}}\right)^N. \tag{21}$$

Again this equation applies to times which provide the same dose using each technique. In this respect, it would be inappropriate to use the treatment times for iso-effective doses which are significantly different. When the same dose is not used, then the respective dose rates (R) can be used instead of treatment times in equation (21), i.e.

$$J = \left(\frac{R_{flash}}{R_{conv}}\right)^N. \tag{22}$$

Geometrical considerations suggest an exponent of 0.33 to represent the event separations within a small volume of 1 μm^3. The typical treatment times quoted by Vozenin (Vozenin *et al* 2019a, 2019b) are around 500 sec for conventional (0.03 Gy sec^{-1}) and around or less than 0.5 sec for Flash effects in the lung, which within equations (24) and (25) (see below) provide a crude solution for N of 0.328, which is strikingly close to the cubed root (0.33) exponent-value for average track separation distances.

For the Pig skin-necrosis data of Vozenin *et al* (2019a, 2019b), there is an apparent isoeffect (or near isoeffect) for 25 Gy at 0.083 Gy per sec. and 34 Gy at 300 Gy per sec. where no late necrosis was found, which implies that these doses are close to the threshold BED value for effectiveness.

With relatively limited data, it is possible to tentatively estimate the entire dose response curves as follows:

1. Apply the cube root function to the dose rates as in equation (26) to change the generally accepted α/β ratio of 3 Gy for skin late effects. The respective treatment dose rates are 300 and 0.083 Gy s^{-1}, so that the FLASH α/β ratio is approximately estimated as

$$\left(\frac{0.083}{300}\right)^{0.3} \times 3 = 35\ Gy \tag{23}$$

   The exponent of 0.3 rather than 0.33 for a cubed root function is used as this was found to give the best fit to the lung fibrosis data set (as in results below).

2. Using the BED threshold (BED_0) concept, then for each treatment condition can be represented by the difference between the full BED and the threshold BED, as follows.

Table 1. Method for OER estimations.

From data of Barendsen (Barendsen *et al* 1966), the cell survival curve of the reference irradiation, with LET of 1.3 keV.μm^{-1}, provides $\alpha = 0.14$ Gy^{-1}, $\beta = 0.04$ Gy^{-2}, and the maximum helium α (α_U) given by 1.07e$^{2.54\alpha}$, and the maximum $\beta(\beta_U)$ by 2β.
The LETU value for oxic cells is 120.6 keV.μm^{-1}, with LET$_U$ for hypoxic cells as 158 keV.μm^{-1}.
The Barendsen data set for OER is based on average OER values from multiple doses. To simplify, the input dose value here is for 3 Gy only for oxic cells.
For each LET value the α, and β value is obtained using the scaling equations for the simple energy efficiency model published elsewhere (Jones 2015), for values less than LET$_U$ as:

$$\alpha_H = \alpha_L + \frac{LETx - LET_C}{LET_U - LETc}.(\alpha_U - \alpha_L)$$

and for values exceeding LET$_U$ as:

$$a_H = \alpha_L + \left(1 - \frac{LETx - LET_U}{LET_x - LET_C}\right).(\alpha_U - \alpha_L)$$

The same equations are used for β.
Values of α and β can then be obtained for oxic and hypoxic cells by using the appropriate LET$_U$ value since α and β must share the same LET$_U$ value to preserve symmetry when dose is increased.
The OER is then found for each LET value by solving for d$_{hyp}$ in the equation which contains suffixes to denote the oxic and hypoxic cells in $\alpha_{ox}\, d_{ox} + \beta_{ox}\, d_{ox}{}^2 = \alpha_{hyp}\, d_{hyp} + \beta_{hyp}\, d_{hyp}{}^2$.
The OER is then d_{hyp}/d_{ox}

Conventional dose rate:

$$D\left(1 + \frac{D}{3}\right) - 25\left(1 + \frac{25}{3}\right) \tag{24}$$

FLASH dose rate:

$$D\left(1 + \frac{D}{35}\right) - 34\left(1 + \frac{34}{35}\right) \tag{25}$$

For the lung fibrosis experiments of Vozenin *et al*, the data set has categorical grades to identify the intensity of fibrosis. By assuming that these grades are multiples of 20 Gy-units of BED (as explained above), the data can be displayed as a relationship between dose and BED*.

Non-linear least-squares fitting is applied to the data to provide α/β values and intercept values using *Mathematica* (Wolfram, Illinois) software.

Also, by assuming that the β related cell kill dominates at high dose, then an estimated of the ratio of $\beta_{\text{flash}}/\beta_{\text{conv}}$ can be obtained for iso-effective doses. The factor J which operates on the changes of the α/β ratios (for conventional and flash irradiations) can then be used to estimate the ratio of $\alpha_{\text{flash}}/\alpha_{\text{conv}}$, by using the following relationships:

The bio-effect (BE) in terms of logarithmic cell kill in the LQ model will be

$$BE = \alpha d + \beta d^2 \tag{26}$$

For an isoeffect, then

$$\alpha_{conv}\, d + \beta_{conv}\, d_{conv}^2 = \alpha_{flash}\, d_{flash} + \beta_{flash}\, d_{flash}^{\ 2} \tag{27}$$

At high dose, the β parameter will dominate such that

$$\beta_{conv}\, d_{conv}^2 = \beta_{\ flash}\, d_{flash}^2 \tag{28}$$

So that

$$\frac{\beta_{flash}}{\beta_{conv}} = \frac{d_{conv}^2}{d_{flash}^2} \tag{29}$$

Equation (20) can be rearranged to estimate of the change in the α parameter as

$$\frac{\alpha_{flash}}{\alpha_{conv}} = \frac{\beta_{flash}}{\beta_{conv}} \times J \tag{30}$$

OER changes

For the estimation of OER changes with LET in Helium ions the method used is given in table 1.

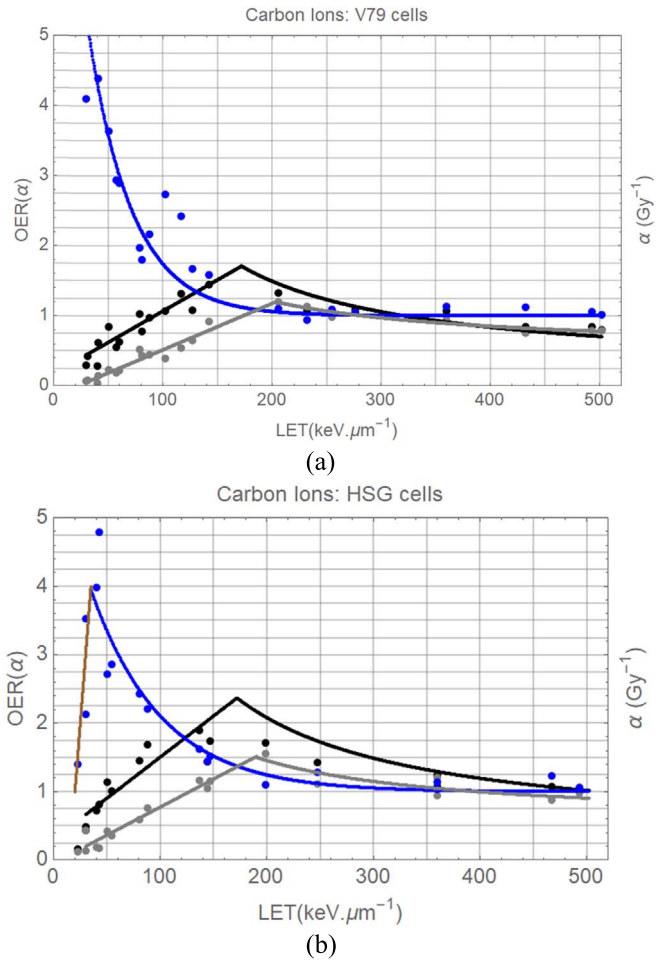

Figure 4. (a) and (b) Relationships between LET and both OER (α) and the α radiosensitivity parameter (a) in V-79 cells and (b) in HSG cells irradiated with carbon ions in oxic (black data points, fitted line and curve) and hypoxic (grey data points and fitted curve) conditions. The blue data points and curve show the change in OER(α) with LET. The brown line in (b) follows an initial steep rise in OER (α) before the progressive fall. (Data from Furusawa *et al* 2000, Furusawa *et al* 2012, no standard errors provided).

Results

Carbon ion data of Furuwasa *et al*

The α parameter radiosensitivites in oxic and hypoxic conditions are plotted for V79 and HSG cells in figures 4(a) and (b) respectively, with the ratio of the α radiosensitivities in oxic and hypoxic conditions plotted as the OER(α). In each figure, the LET_U for hypoxic cells exceeds that for oxic cells and the maximum value of α is lower for the hypoxic cells. The OER(α) ratio falls sharply from high values (exceeding the standard OER) and asymptotically approach unity at higher LET values. There is a suggestion, only visible in the HSG cell data (figure 4(b)), that this ratio may initially increase at low LET values before it reduces. Although such a finding may be spurious, it is realistic since the rapid initial increase in oxic radiosensitivity with LET will be greater than the initial increase in the hypoxic radiosensitivity (due to their different LET_U or peak values).

The results for neon ions are shown in figures 5(a) and (b). These are remarkably similar to the carbon ion results except for the higher values of LET_U. Again, the hypoxic LET_U values exceed those for oxic cells and the highest α values occur in oxic cells. There is also one data point which shows a low OER(α) ratio at the lowest LET values in V79 cells (figure 5(a)) and is compatible with an initial sharp rise followed by the reduction.

The average percentage change in the LET_U position for hypoxic cells compared with the oxic cells is plotted for different ion Z values from the data sets (C, Ne and He ions) (Barendsen *et al* 1966, Furusawa *et al* 2000, Furusawa *et al* 2012), and is found to fit the function

$$15 + e^{0.264 \times Z} \tag{31}$$

These results are shown in figure 6, where the data points are in blue, with other Z values obtained using equation (31).

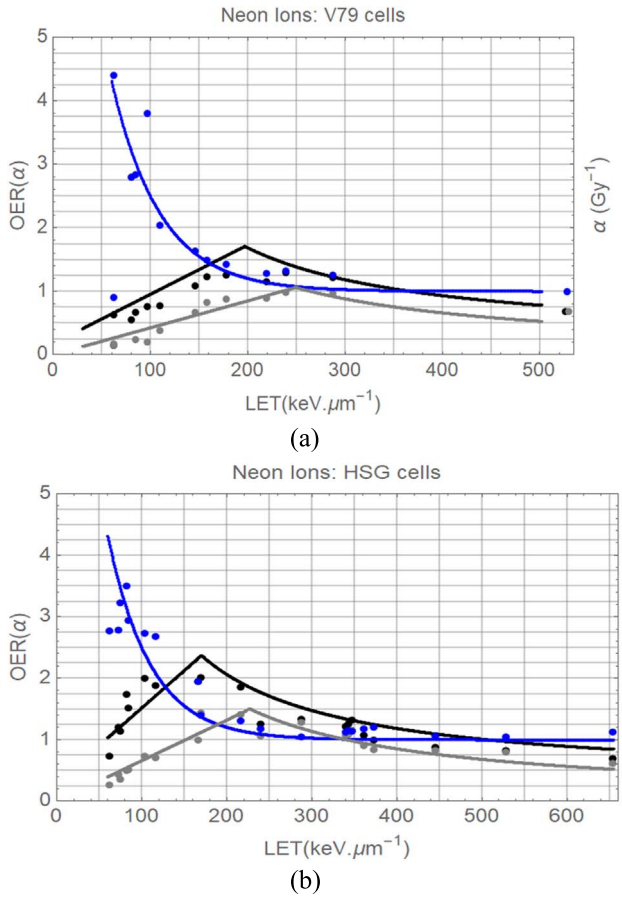

Figure 5. (a) and (b) Relationships between LET and both OER(α) and the α radiosensitivity parameter (a) in V-79 cells and (b) in HSG cells irradiated with neon ions in oxic (black data points, fitted line and curve) and hypoxic (grey data points and fitted curve) conditions. The blue data points and curve show the change in OER(α) with LET. (Data from Furusawa *et al* 2000, Furusawa *et al* 2012, no standard errors provided).

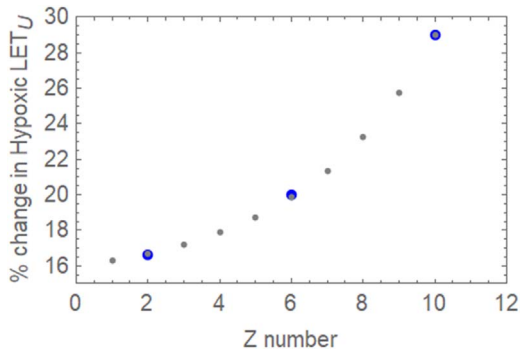

Figure 6. Plots of average percentage change in hypoxic LET_U (relative to the oxic LET_U) are shown for Helium($Z = 2$), Carbon ($Z = 6$) and Neon($Z = 10$) as blue points with modelled estimates using the exponential function as grey points.

These data and the assumptions made above are used to predict the results found by Barendsen *et al* (Barendsen *et al* 1966), as shown in figure 7. When considering the multiple experiments involved in OER determination and the influence of biological variation (which can amount to coefficients of variation of 30% (Jones 2021)), these estimates are reasonably satisfactory for LET values up to 100 keV.μm^{-1} but with greater inaccuracy, although following the same trend, at higher LET values.

Protons

Application of equation (12) is used to estimate the modified LET_U values for protons when time is reduced by a time reduction factor ratio as shown in figure 8. An unmodified exponent of 0.33 was used to incorporate the

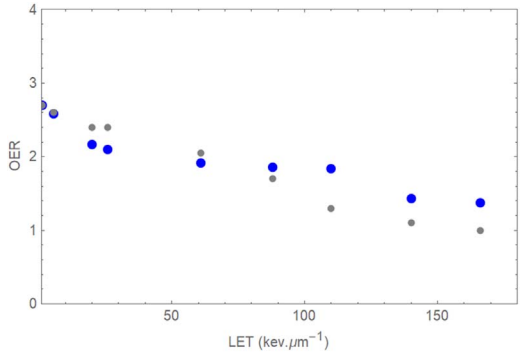

Figure 7. OER data for helium ions published by (Barendsen *et al* 1966) are shown as grey points. Modelled predictions using methods given in table 1 are shown as blue points.

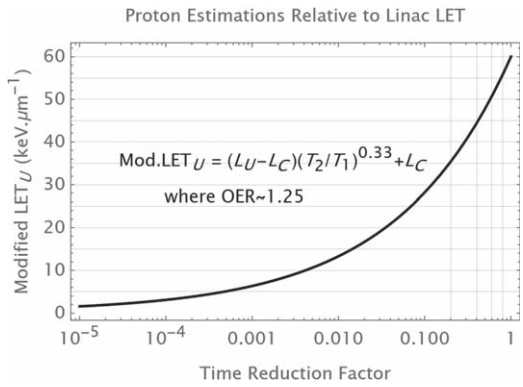

Figure 8. Plot of the estimated change in LET_U position for protons with changes in the time reduction factor (T_2/T_1) by use of the function shown on the graphic.

micro-volume concept. A time reduction factor of 10^{-2} or 10^{-3} is sufficient for major reductions in LET_U values. Since the OER is around 1.25 at LET_U, it is reasonable to assume that the curve displayed will represent such an OER value. Accordingly, significant reductions in OER can be expected with increased dose rates of these orders of magnitude, as might be found in proton FLASH irradiations.

The dose rate and fluence rate issues described above may have subtle consequences for standard proton treatments. For example, even if linac and cyclotron treatment times are apparently isochronous, due to scanning there will be an effective halving of the treatment time, since in mid-volume the dose is delivered in half of the time, so that a slight correction to RBE estimations can be made by applications of equation (13).

To provide a mechanistic interpretation of these results, figures 9(a) and (b) should be closely compared as they show the estimated shifts of the oxic and hypoxic LET and OER relationships for proton irradiations at standard and FLASH dose rates respectively. The information shown in figure 6 has been used to set the LET_U values and the time reduction factor of 10^{-2} applied.

For protons at 'high' fluence rates the LET_U positions, seen in figure 9(b), are predicted to shift to much lower values. Although RBE will be expected to increase, it will be inversely dependent on the dose per fraction and so may not be apparent in high dose *in vivo* experiments and will further reduce due to induced hypoxia when compared to the standard dose rate condition.

BED method results

For the published data sets which compare conventional dose rates and FLASH (van Rongen *et al* 1993, Jones and Dale 2018), the following results were obtained

Figure 10(a) shows the least-squares fitted lung fibrosis data for conventional and Flash conditions respectively, with solutions for the α/β ratio and C, the intercept BED. C is the BED at (near) zero dose, but the tissue radiation damage effects will only occur after the threshold BED has been exceeded. The fitted parameters, with uncertainties, are given in:

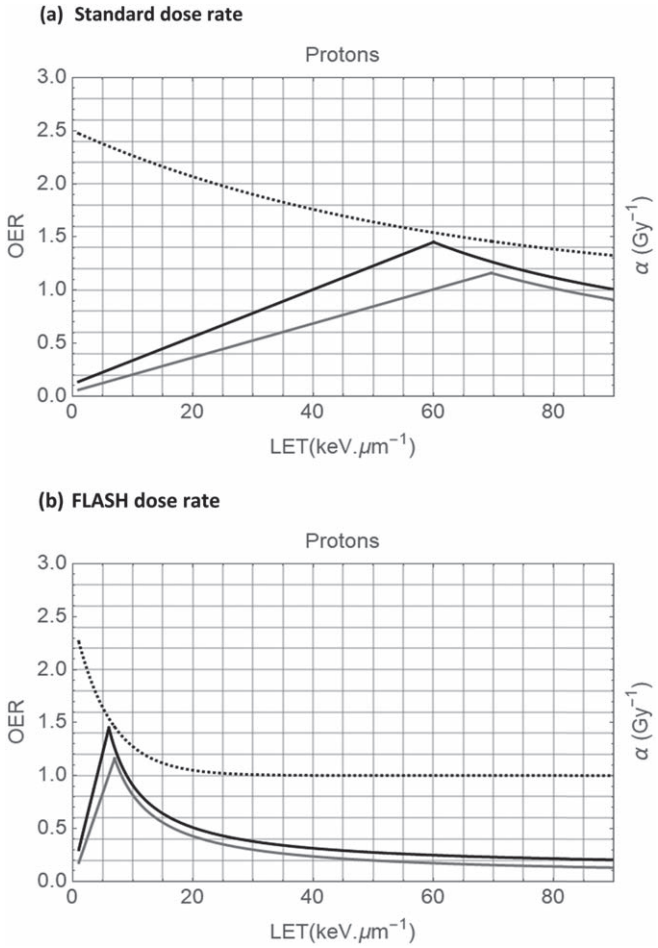

Figure 9. (a) and (b) Speculative graphic showing OER(α) and α parameters for protons in oxic (black) and hypoxic (grey) conditions. Graphic (a) is at a standard dose rate where the oxic and hypoxic LET_U is around 60 and 69 keV.μm^{-1} respectively. The OERα (dashed curve) is high in the standard LET range of 1–10 keV.μm^{-1}, with a value of around 2.4 at a LET of 5 keV.μm^{-1}. In (b) with a time reduction factor of 10^{-2}, the proton oxic and hypoxic LET_U are both below 10 keV.μm^{-1} respectively. The OER(α) is around 1.6 at the LET of 5 keV.μm^{-1}.

$$CONV\text{: } BED^* = d\left(1 + \frac{d}{3.4}\right) - 44,\ R^2 = 0.95,\ overall\ p = 0.05.$$

$$FLASH\text{: } BED^* = d\left(1 + \frac{d}{32.74}\right) - 16.55,\ R^2 = 0.93,\ \ overall\ \ p < 0.01.$$

The α/β of 3.4 Gy found with a conventional dose rate is typical for murine lung fibrosis (the expected value is 3–4 Gy (van Rongen *et al* 1993)), but the flash-elevated α/β of 32.74 Gy suggests hypoxia due to a net reduction in β by the OER in the presence of an elevated α due to increased volumetric ionisation clustering which increases α substantially but with lesser increments in β (Jones 2015). It is also known that hypoxia-induced reductions in α are less than those affecting the β parameter (see appendix), so that the α/β ratio will probably increase for these two reasons. There can be no effect on cell-cycling related radiosensitivity changes during very rapid irradiation. Also, the longer term enzymatic DNA-repair processes which influence β are negligible at very short treatment times.

The fitted α/β ratios of 3.4 and 32.74 Gy can then be used to check the cubed root of time function. The dose rates 60 Gy sec^{-1} and 0.03 Gy s^{-1}. The cubed root function J (equation (26)), which will operate on radiosensitivity changes will then be approximately:

$$J = \sqrt[3]{\frac{60}{0.03}} = 12.38, \tag{32}$$

which is larger than the change in α/β ratios of 9.63 ($F = 32.74/3.4 = 9.63$) found from the data set fitting. For a more similar result an exponent of 0.3, rather than 0.33 for the cubed root, provides a J-value of $(60/0.03)^{0.3} = 9.78$.

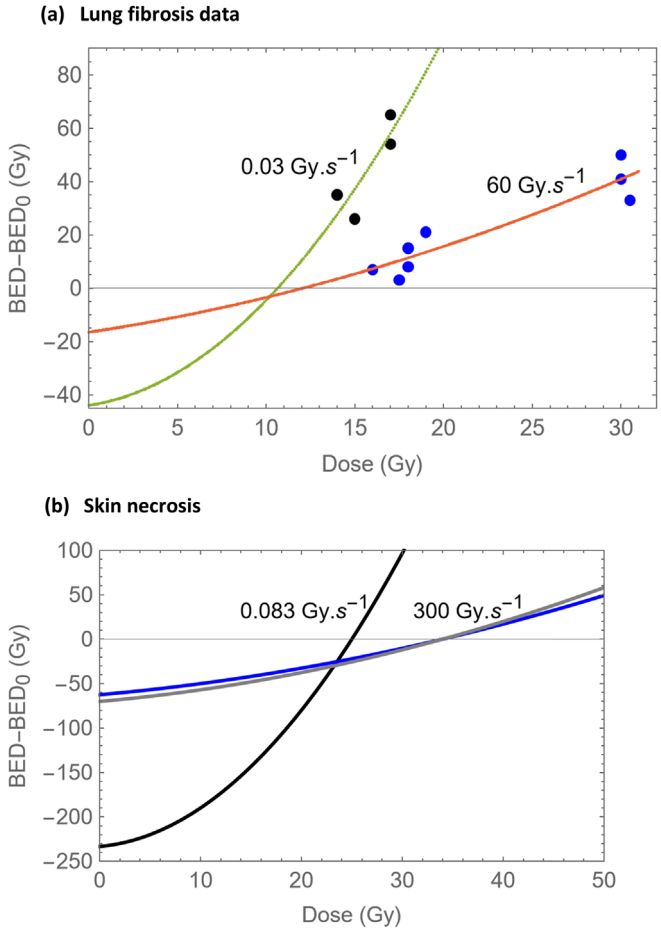

Figure 10. (a) and (b) Graphic of plots of BED*(= BED–BED$_0$), using fitted lines to data sets of Vozenin *et al* (a) for data of murine lung fibrosis where black points = CONV (0.03 Gy. s^{-1}); blue points=FLASH (60 Gy.s^{-1}), with fitted curves and (b) pig skin necrosis where continuous functions are used to match the two iso-effects using equations (28) and (29) at the threshold doses of 25 and 34 Gy, using two assumptions for the volumetric effect: exponent of 0.30 for the grey curve and 0.33 for the blue curve. The fitted parameters are given in the text.

Thus the conventional dose rate α/β of 3.4 Gy, when multiplied by F, provides a Flash α/β of 3.4 Gy $\times 9.77 = 33.22$ Gy, which is remarkably close to the fitted value of 32.74 Gy. More data could help solve the uncertainty in this region of the dose response curves.

Furthermore, the lung fibrosis isoeffects found at around 15 and 30 Gy provides an estimate of the overall reduction in β, as $15^2/30^2 = 0.25$, which in turn suggests an estimated α parameter increment of $0.25 \times 9.77 = 2.4$ approximately (using equations (32)–(34)).

The skin necrosis data (Jones *et al* 2001, Vozenin *et al* 2019b) has only two apparent isoeffects, both at the threshold dose (or very close to it), although the flash data being the highest dose when no effect was seen (therefore including some uncertainty). Equations (28) and (29) (see methods) are plotted in figure 10(b), where the two experimental isoeffective threshold doses of 25 and 34 Gy fall on the zero line. Such plots may be helpful to guide future experiments where skin necrosis can be obtained, although no uncertainties are available. The variation introduced to the exponents which provides F (from 0.30 to 0.33) produces little change in the BED plots for α/β ratios of 32 and 40.5 Gy respectively

The estimated $\beta_{flash}/\beta_{conv}$ ratio for the skin data is $25^2/34^2 = 0.54$, which with an α/β value factor change of around 11.7, gives an estimated $\alpha_{flash}/\alpha_{conv}$ of $0.54 \times 11.7 = 6.32$. Should even higher FLASH doses result in no effect, then this value would be lower and could approach that obtained for the lung fibrosis data.

The resultant high $(\alpha/\beta)_{flash}$ value allows far less change in tissue effect with increasing dose (or BED) compared with the conventional situation, resulting in the crossing-over effect seen in the curves shown in figure 10(b) despite the flash curve being much closer to the tolerance level initially owing to the higher α radiosensitivity.

Discussion

The above methods have provided an overall relationship between very high dose rates and changes in micro-volumetric LET, and the modification of radiosensitivity by the oxygen effect.

The depletion of oxygen with increasing dose and dose rate was inferred in the early 1970s by Berry (Berry and Stedeford 1972) and others (Wilson *et al* (Wilson *et al* 2012) has reviewed the early literature). The later work of Ling included more detailed studies linking oxygen status to repair capacity at lower dose rates (Ling 1975, Ling *et al* 1988). However, some recent studies have produced scepticism about the role of oxygen depletion and consequently they need considerable discussion. For example, the study by Jansen *et al* (2021) depended on earlier chemical work by Mihaljevic *et al* for linoleic acid peroxidation as a biomimetic model of free radical reactivity (Mihaljević *et al* 2011). The process under study involved additional molecular changes in lipids, and in the presence of reactive thiols which negate rapid radiation effects. They assume an initial high level of oxygen and steady state approximations for subsequent products, and so may not be suitable for FLASH or ultra-high dose effects where existing hypoxia appears to be necessary. Such experiments cannot measure oxygen changes close to radiation tracks. Also, the publications of Cao *et al* (2021) did find some limited oxygen depletion at very high dose rates.

Critiques of these two publications (Cao *et al* 2021, Jansen *et al* 2021) can be expressed as:

1. Most *in vitro* work was done at 23–25 degrees Celsius and not at body temperature; so may not yield as many radiolysis products with oxygen depletion as would occur at 37 degrees Celsius.
2. The techniques used oxygen sensors which have long capture times in excess of 400 msec, whereas the oxygen sensitisation mechanism is complete within 30 msec.
3. Cao *et al* (2021) gives caveats due to experimental technical limitations. Their maximal sampling rate was around 150 ms per measurement, far exceeding oxygen sensitisation mechanism which is complete in 30 ms and where FLASH 20 Gy doses were given in around 74 msec; Jansen *et al* fails to mention these aspects.
4. Cao *et al* explain that the sampled volume, of 100–150 mm^3, are appropriate for aqueous solutions (they used bovine serum albumen also) and not for tissues, and they quote a 'blind time' of 450 microseconds. They have uncertainties about oxygen concentrations at shorter times (nanoseconds to microseconds) required for the fundamental physico-chemical reactions (Watts *et al* 1978, Wardman 2009). Time pulses used for FLASH techniques can be shorter than this 'blind time'. Other factors mentioned are the oxygen electrode specificity, and that 'The gap of 450 msec in oxygen sampling prevented quantification of the actual extent of oxygen depletion'. They also suggest that the lack of dependence on dose rate found might be due to signal-to-noise issues. However, their findings of 1–3 mm Hg oxygen partial pressure changes would be sufficient to change the radiosensitivity of already hypoxic tissues, although their yields may be seriously underestimated due to the above limitations.
5. The work of Jansen *et al* used *G* values at around 25 degrees Celsius in water. They also used ph7 de-ionised water, and not ionised physiological water. Hypoxic biological conditions are accompanied by a low pH (acidosis), which also influences radiosensitivity (Röttinger and Mendonca 1982). The results of Jansen *et al* clearly show saturation of oxygen yield in a large volume with increasing dose rate (their figure 5); but that does not exclude very rapid and more substantial oxygen depletion in small volumes over a time scale relevant to FLASH effects .
6. It is important that the most relevant spatial scales are considered. The oxygen depletion will only occur near to radiation tracks, and are relevant for short time intervals (up to 30 milliseconds). There will also be equilibration of oxygen from greater distances. Thus the extent of oxygen depletion over a large volume will not well-reflect the short term changes close to radiation tracks.

For the above reasons, these experiments probably do not adequately represent the conditions at which FLASH effects operate *in vivo*, and specifically for small changes in oxygen tension in pre-existing hypoxia over smaller durations of time.

The proposed model in the current paper considers 1 μm^3 volumes, in which the *S* and *S*′ distances reduce with increased dose rate, a biologically realistic situation for very high dose rate effects.

In the present paper, the graphical finding that LET-RBE (and radiosensitivity) turnover points will occur at higher LET_U values for hypoxic than oxic cells with conventional dose rates is probably because the increase in radiosensitivity with LET will be less efficient in hypoxic cells owing to the reduced yield of damaging oxidative species present (Wardman 2009). There is supporting evidence in that yields of DSB and more complex DSB change as a function of LET and oxygen status (Strigari *et al* 2018, Hanton *et al* 2019, Hughes and Parsons 2020).

The links between fluence rate (and not total fluence), instantaneous dose rate and treatment exposure duration may not be so obvious, but the distinction is important. It must be remembered that, for the same dose, low fluence rates require longer exposure times to provide the same number of photons or charged particles, and that they will not be so 'concentrated' in time, with greater *S* and *S'* distances. Conversely, high fluence rates require shorter exposure times, accompanied by a 'denser' number of particles per unit volume with closer inter-track distances resulting in more clustered DNA damage. The rapid fundamental physico-chemical interactions can be modified by the redox potential of the aqueous medium and also by radio-protective compounds many of which are naturally occurring, such as sulphydryl groups, ascorbic acid and others (Wardman 2009). The degree of complexity, due to ionisation clustering, of DNA damaged sites increases with LET; a similar effect occurs with increasing dose rate. Hence, micro-volumetric interpretations of LET, such as mVET, are necessary to quantify the energy transfer obtained in small volumes during small intervals of time when the fluence rate has increased. In essence, FLASH dose rate effects mimic high-LET, and can be considered quasi high-LET, but with enhanced oxygen depletion sufficient to reduce overall bio-effectiveness at high dose per fraction.

It is axiomatic that as both LET and fluence rate increase, the radiosensitivity increase per unit LET will be more efficient than at lower fluence rates. This effect will inevitably increase the increment in RBE per unit LET, which must reach a maximum saturation level before the process becomes inefficient due to overkill and wasted energy (Jones 2015). Thus, LET_U must shift to lower LET values when fluence rates increase. The oxic and hypoxic radiosensitivity values will both increase more efficiently with LET, resulting in their turnover peaks occurring at lower LET_U values. There will also be a dissociation between the net changes in both α (which increases, although to a lesser extent in hypoxia than in oxic conditions) and β (which decreases substantially with oxygen depletion).

Thus, it is rational to expect that very high fluence rates will cause a significant reduction in the OER even at lower LET values (since the LET will not have changed, but the mVET will have changed considerably). Such changes will be associated with an increase in RBE but this will be considerably modified by the oxygen depletion. Since RBE is inversely dependent on dose per fraction (Jones 2015) there will be some reduction in RBE when large doses are used (as occurs in *in vivo* experiments which use single fractions). Thus, although the FLASH effect is similar to an increase in LET, the accompanying changes in the β-related OER will be sufficient to oppose the increase in RBE and increase the radio-tolerance of a tissue.

The degree of change of biological effect should vary with collimation and beam delivery technique. Inverse square law effects apply for scattered beams, even with longer source skin distances (SSD). For example, an SSD of 100 cm will have reductions given by $100^2/(100 + \text{depth})^2$, which for depths of 2, 5, 10 and 20 cm are respectively 0.90, 0.83, 0.76, 0.69. The inevitable reduced dose rate with depth is less than an order of magnitude. For an exposure of one minute, the change in inter-track distances will be by factors of 1.05, 1.1, 1.5 and 1.2 respectively which is unlikely to have significant effects, but these may to some extent be opposed by the limited beam softening which occurs with increasing depth in megavoltage photon beams due to the change in photon wavelength (and energy) due to Compton scattering, a factor which is not usually considered in RBE studies; there is scope for further research on this issue in depth-related RBE studies.

Synchrotron 'light sources' produce very high dose rates using linear photon micro-beams (with energies typically between 70 and 150 keV) with no inverse square law fall off due to divergence. These require little dose rate correction with depth, apart from the reduced dose and dose rate due to electron interactions and energy loss along the beam. Very high normal tissue tolerance doses have been found as with FLASH and tumour control responses have been encouraging (Bobyk *et al* 2012).

Although some of the above work is speculative, the hypotheses presented are experimentally testable, e.g. the α and β changes with mVET and fluence rates. These, if confirmed, would place ultra-high dose rate or FLASH effects on a more rational basis. There is presently considerable research in this area.

There remains a huge variation in the dose rates at which cellular *in vitro* and tissue *in vivo* ultra-high dose rate experimental outcome changes are seen (Berry and Stedeford 1972, Ling 1975, Wilson *et al* 2012). *In vitro* experiments use far lower dose exposures due to the dependency of survival fraction experiments on surviving colony numbers, and irradiations normally occur in optimal growth conditions. In contrast, *in vivo* experiments contain intact tissues containing variable, often phasic, redox potentials with suboptimal amounts of radio-protective agents. Normal tissues have phasic blood flow dynamics, depending on their functional requirements.

In vivo FLASH experiments use large single fractions, where RBE will be low, but have the radio-protective advantage of the reduced OER, thus increasing overall radio-tolerance. Changing to lower fractionated FLASH doses is predicted to give higher RBE values which may compensate for the advantages of the lowered OER. Future experiments should be guided by realistic models concerned with dose per fraction, changes in OER and radio-tolerances. This forms a large research prospectus.

Further issues that may influence the threshold to achieve ultra-high dose rate effects are physical, including beam-related parameters such as beam energies which for charged particles will influence the inter-track distances (*S*) depending on particle energy, velocity, mass and charge. Thus electrons having low mass and unit charge will separate more effectively than would heavier ions and especially at lower energies. It is therefore likely that electrons (when at a sufficiently low energy) will have larger *S* values and therefore require far higher dose rates.

The classical ultra-high dose rate *in vitro* experiments summarised in Wilson *et al* (Wilson *et al* 2012), had a dose rate requirement of around 10^9 Gy per second and a minimum threshold dose of at least 5 Gy to deplete oxygen sufficiently in pre-existing low oxygen conditions. To achieve such effects an exponent value of around 0.12 is required in equation (12). Experimental verification of the exponent values for different ion beams at different energies is indicated and may provide useful information, as might Monte Carlo simulation studies. However, in the classical ultra-high dose rate experiments (Wilson *et al* 2012), uncertainty was admitted about the pulse structure and dosimetry (Berry and Stedeford 1972), with potential systematic errors amounting to several orders of magnitude, although the relative effects would remain valid. This does mean that the cubed root function should not be applied to these data sets because of the uncertainty about the actual dose rates. Another issue is that P338 leukaemia cells were used in one data set (Berry and Stedeford 1972). These have linear cell survival curves indicating a very small β parameter at conventional dose rates, indicating a high intrinsic α/β ratio, so that much higher dose rates than in FLASH experiments might be required.

There is also a need to have standard reference definitions for all controllable experimental conditions in dose rate experiments. Experiments need to be designed to show biological isoeffects at different combinations of dose and dose rate in order to facilitate model building. Most extant publications do not provide such information and greater precision as to threshold doses for FLASH effects is required.

Small animal and human radiobiological studies differ significantly in terms of dose-fractionation. The use of high single-dose experimental exposures with hypoxic cell sensitizers did produce promising results in small animals, but disappointing results when applied with much lower fractionated doses in humans (Dische 1991). Similar outcomes occurred in high pressure oxygen or hyperbaric oxygen trials (Radiotherapy and hyperbaric oxygen 1978) when compared with animal studies. Thus, considerable care needs to be taken if extrapolating ultra-high dose rate effects from animal experiments to humans.

The potential advantage of a reduced OER with Carbon and other ions has been discussed by various authors, especially the effect of spreading out the Bragg peaks which inevitably reduces the reduction in OER (Suit *et al* 2010, Antonovic *et al* 2015, Wenzl and Wilkens 2011, Tinganelli and Durante 2020). Ultra-high dose-rates and FLASH deliberately reduces the OER which may protect normal tissues which exhibit physiological forms of phasic hypoxia. At least part of the anti-tumour effect may be due to further depletion of oxygen in already hypoxic cells, with oxygen diffusion from blood vessels requiring over 10 seconds to cover 150 μm distances from tumour blood vessels (Wilson *et al* 2012).

More comprehensive experimental studies are necessary for obtaining useful statistical uncertainties which should be included in data sets, although often not so (Furusawa *et al* 2000, Furusawa *et al* 2012, Vozenin *et al* 2019a).

For example, studies by Tinganelli *et al* contain only two different LET vales for C ions and one LET value for O_2 and N ions (Tinganelli *et al* 2013), and only limited LET ranges (Tinganelli *et al* 2015), although the OER reductions are consistent with those in the present study. The requirements for more comprehensive experiments, including detailed microdosimetry and variations around the oxygen tension, are self-evident.

Much research work is necessary to clarify the mechanisms and dynamics in preparation for proposed clinical studies of higher dose rates using protons and heavier ions. Existing scanned beam protons may also, in principle, confer some degree of radioprotection in pre-existing hypoxic normal tissues, a topic worthy of research.

At present, there are many competing mechanisms for FLASH effects (Berry and Stedeford 1972, Ling 1975, Wilson *et al* 2012, Hanton *et al* 2019, Vozenin *et al* 2019a, Hughes and Parsons 2020), although transient localised oxygen depletion remains the most likely. The review of FLASH radiotherapy by Hughes *et al* is comprehensive, including alternative but less likely mechanisms than oxygen depletion (Hughes and Parsons 2020). There are also technical limitations to the presently achievable dose rates for ion beams, although physicists are currently addressing these issues (Jolly *et al* 2020).

Conclusions

The relationships between fluence rates, dose rates (and radiation exposure times) and the faster accumulation of energy in small volumes are capable of changing radiosensitivites in oxic and hypoxic conditions. High fluence rates, with short treatment times, will cause sufficient oxygen depletion in hypoxic sites to change

radiosensitivity, although at LET values considered to be low. A more volumetric interpretation of LET is required and a considerable body of research must be undertaken to study changes in LET-RBE turnover points with dose rate in oxic and hypoxic conditions, with dose rate increases in particle and photon beams. The BED method may be very useful in this respect since the key α/β biological parameter is increased in proportion to the fluence (or dose) rate changes.

Acknowledgments

Drs M Hill, R Dale, G Royle, A Poynton, A Kacperek, C Tsuey, B Vojnovic, P O'Neil and P Wardman are all thanked for discussions on this theme in recent years. This work is not grant funded.

Conflicts of interest

There are no conflicts of interest.

Appendix A

OER was strictly defined by Alper (Alper 1979) as the ratio of doses to obtain an isoeffect in the presence and absence of oxygen, that is between oxic and anoxic conditions. RBE is the ratio of doses to obtain an isoeffect for a reference radiation of low LET and a test radiation of higher LET (the oxygenation status is unspecified). For megavoltage x-rays (MVX-R) and an unspecified particle (P) it is self-evident that, for typical RBE values the anoxic RBE must exceed that of the oxic RBE, as shown in figure A1 where the values are approximately: OER (MVX-R) $=$ 2; OER(P) $=$ 1.5; RBE(anoxic) $=$ 2.4; RBE(oxic) $=$ 2.15.

Alper also stated that 'oxygen is consumed in radiation chemical reactions, so a constant partial pressure can only be maintained only if the rate at which it is supplied to the irradiated system is a least sufficient to balance the rate of its consumption, which in turn will be governed by the dose rate.' This was most apparent at low partial pressures of oxygen in an experiment.

Studies using photons of various energies have shown larger OER values for β (typically OER$\beta = 3.25$) than for α (OER$\alpha = 1.75$) which leads to a reduced overall OER at low dose per fraction where α related cell-kill predominates (Jones *et al* 2007). At high dose per fraction the β value will dominate, resulting in a higher overall OER. It follows that in hypoxic states (and with oxygen depletion from whatever mechanism) that there will be less separation of the survival curves between anoxia and the hypoxic state than between the oxic and the anoxic state, thus lowering OERβ, and lead to a large reduction in β compared to the oxic β value.

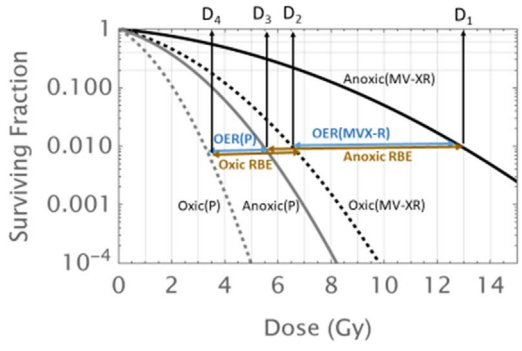

Figure A1. Modelled Survival curves for megavoltage x-rays (MVX-R) and a particle radiation (P) for irradiations in anoxic and oxic conditions. The arrows point to isoeffective doses in the various conditions, from which OER and RBE are found. The radiobiological ratios are: OER (MV-XR) $= D_1/D_2$; Anoxic RBE $= D_1/D_3$; OER (P) $= D_3/D_4$; Oxic RBE $= D_2/D_4$.

Appendix B

Definitions: average inter-track distance $= S$; inter-track significant damage event distance $= S'$.

In two dimensions, S^2 (the average area which contains one track) depends inversely on fluence (F), which is the ratio N/A, where $N =$ track numbers and A the cross sectional area, so that

$$S^2 = \frac{A}{N} = \frac{1}{F}.$$

The linear dimension for S is then $\sqrt{\frac{1}{F}}$.

For S' distances in a volume there are further considerations. Since the total energy per unit volume is $mVET = F \times LET$, it is assumed that in some cubic volumes there will be up to P events where P is proportional to

$\frac{mVET}{C}$, where C is the averaged energy requirement for each such event.

It follows that the average volume which contains a single significant event is proportional to

$$\frac{1\mu m^3}{P} = \frac{C}{mVET} = \frac{C}{F \times LET}.$$

The average linear separation distance of such events, S' is then proportional to

$$\sqrt[3]{\frac{C}{F \times LET}},$$

indicating that S' is inversely proportional to the cubed root of fluence.

For the comparisons of ratios of different S' values (e.g. S_1' and S_2' due to variations in fluence or dose rates (referred to as *rate*), or treatment times designated by the same subscripts), then where C and LET, and any other associated functions, are the same these terms will cancel out, and

$$\frac{S_1'}{S_2'} = \sqrt[3]{\frac{F_2}{F_1}} = \sqrt[3]{\frac{rate_2}{rate_1}} = \sqrt[3]{\frac{T_2}{T_1}}$$

(provided that the same dose is given in the case of time).

It is acknowledged that there will be large variations of energy deposition for any particular LET value, such that some cubic volumes will have very few significant events which may not lead to lethality, but others a higher number, some sufficient to cause chromosomal breakage and cell death, but the overall proportionality will hold based on the mean LET value along a track: higher LET values will inevitably be associated with more events and lead to a higher probability of causing cellular lethality.

ORCID iDs

Bleddyn Jones https://orcid.org/0000-0002-6698-1660

References

Alper T 1979 pages 50 and 55-56, chapter 6 (Radiosensitisation by oxygen)*Cellular Radiobiology* (Cambridge: Cambridge University Press)

Antonovic L, Dasu A, Furusawa Y and Toma-Dasu I 2015 Relative clinical effectiveness of carbon ion radiotherapy: theoretical modelling for H&N tumours *J. Radiat. Res.* **56** 639–45

Barendsen G W, Koot C J, van Kersen G R, Bewley D K, Field S B and Parnell C J 1966 The effect of oxygen in impairment of the proliferative capacity of human cells in culture by ionizing radiations of different LET *Int. J. Radiat. Biol. Related Studies Phys. Chem. Med.* **10** 317–27

Berry R J and Stedeford J B H 1972 Reproductive survival of mammalian cells after irradiation at ultra- high dose-rates further observations and their importance for radiotherapy *Br. J. Radiol.* **45** 171–7

Bobyk L *et al* 2012 Intracerebral delivery of carboplatin in combination with either 6 MV photons or monoenergetic synchrotron x-rays are equally efficacious for treatment of the F98 rat glioma *J. Exp. Clin. Cancer Res.* **31** 78

Britten R A *et al* 2013 Variations in the RBE for cell killing along the depth-dose profile of a modulated proton therapy beam *Radiat. Res.* **179** 21–8

Calugaru V, Nauraye C, Noel G, Giocanti N, Favaudon V and Megnin-Chanet F 2011 Radiobiological characterization of two therapeutic proton beams with different initial energy spectra used at the institut curie proton therapy center in orsay *Int. J. Radiat. Oncol. Biol. Phys.* **81** 1136–43

Cao X *et al* 2021 Quantification of oxygen depletion during FLASH irradiation in vitro and in vivo *Int. J. Radiat. Oncol. Biol. Phys.* **111** 240–8

Dische S 1991 A review of hypoxic cell radiosensitization *Int. J. Radiat. Oncol. Biol. Phys.* **20** 147–52

Furusawa Y *et al* 2000 Inactivation of aerobic and hypoxic cells from three different cell lines by accelerated (3)He-, (12)C- and (20)Ne-ion beams *Radiat. Res.* **154** 485–96

Furusawa Y *et al* 2012 Erratum *Radiat. Res.* **177** 129–31

Hanton F *et al* 2019 DNA DSB repair dynamics following irradiation with laser-driven protons at ultra-high dose rates *Sci. Rep.* **9** 4471

Hughes J R and Parsons J L 2020 FLASH radiotherapy: current knowledge and future insights using proton-beam therapy *Int. J. Mol. Sci.* **21** 6492
Jansen J *et al* 2021 Does FLASH deplete oxygen? Experimental evaluation for photons, protons and carbon ions *Med. Phys.* **48** 3892–990
Jolly S, Owen H, Schippers M and Welsch C 2020 Technical challenges for FLASH proton therapy *Phys. Med.* **78** 71–82
Jones B 2015 A simpler energy transfer efficiency model to predict relative biological effect (RBE) for protons and heavier ions *Front. Oncol.* **11** 460–80
Jones B 2017 Particle physics for biological interactions Chapter 1 (1.5—1.15) *Practical Radiobiology for Proton Therapy Treatment Planning.* (Bristol and Philadelphia: Institute of Physics Publishing) 5-4-5-7
Jones B 2021 Fast neutron energy based modelling of biological effectiveness with implications for proton and ion beams *Phys. Med. Biol.* **66** 045028
Jones B, Carabe-Fernandez A and Dale R G 2007 The oxygen effect chapter 8 *Radiobiological Modelling in Radiation Oncology* ed R G Dale and B Jones (London: British Institute of Radiology Publishing) pp 138–57
Jones B and Dale R G 2018 The evolution of practical radiobiological modelling *Br. J. Radiol.* 20180097
Jones B, Dale R G, Deehan C, Hopkins K I and Morgan D A L 2001 The role of biologically effective dose (BED) *Clin. Oncol. Clin. Oncol.* **13** 71–81
Jones B and Hill M A 2019 Physical characteristics at the turnover-points of relative biological effect (RBE) with linear energy transfer (LET) *Phys. Med. Biol.* **64** 225010
Jones B and Hill M A 2020 The physical separation between the LET associated with the ultimate relative biological effect (RBE) and the maximum LET in a proton or ion beam *Biomed. Phys. Eng. Express* **6** 055001
Jones B, McMahon S J and Prise K M 2018 The radiobiology of proton therapy: challenges and opportunities around relative biological effectiveness *Clin. Oncol. (R Coll Radiol).* **30** 285–92
Ling C C 1975 Time scale of radiation-induced oxygen depletion and decay kinetics of oxygen-dependent damage in cells irradiated at ultrahigh dose rates *Radiat. Res.* **63** 455–67
Ling C C, Robinson E and Shrieve D C 1988 Repair of radiation induced damage -dependence on oxygen and energy status *Int. J. Radiat. Oncol. Biol. Phys.* **15** 1179–86
Mihaljević B, Tartaro I, Ferreri C and Chatgilialoglu C 2011 Linoleic acid peroxidation versus isomerization: a biomimetic model of free radical reactivity in the presence of thiols *Org. Biomol. Chem.* **9** 3541–8
Radiotherapy and hyperbaric oxygen 1978 Report of a medical research council working party *Lancet* **2** 881–4
van Rongen E, Thames H D and Travis E L 1993 Recovery from radiation damage in mouse lung: interpretation in terms of two rates of repair *Radiat. Res.* **133** 225–33
Röttinger E M and Mendonca M 1982 Radioresistance secondary to low pH in human glial cells and Chinese hamster ovary cells *Int. J. Radiat. Oncol. Biol. Phys.* **8** 1309–14
Strigari L, Torriani F, Manganaro L, Inaniwa T, Dalmasso F, Cirio R and Attili A 2018 Tumour control in ion beam radiotherapy with different ions in the presence of hypoxia: an oxygen enhancement ratio model based on the microdosimetric kinetic model *Phys. Med. Biol.* **63** 065012
Suit H *et al* 2010 Proton versus carbon ion beams in the definitive radiation treatment of cancer patients *Radiother. Oncol.* **95** 3–22
Tinganelli W *et al* 2013 Influence of acute hypoxia and radiation quality on cell survival *J. Radiat. Res.* **54** i23–30
Tinganelli W *et al* 2015 Kill-painting of hypoxic tumours in charged particle therapy *Sci. Rep.* **5** 17016
Tinganelli W and Durante M 2020 Carbon ion radiobiology review *Cancers (Basel)* **12** 3022
Vozenin M C *et al* 2019b The advantage of FLASH radiotherapy confirmed in mini-pig and cat-cancer patients *Clin. Cancer Res.* **25** 35–42
Vozenin M-C, Hendry J H and Limoli C L 2019a Biological benefits of ultra-high dose rate FLASH radiotherapy: sleeping beauty awoken *Clin. Oncol. (R Coll Radiol)* **31** 407–15
Waligórski M P R, Grzanka L and Korcyl M 2015 The principles of Katz's cellular track structure radiobiological model *Radiat. Prot. Dosim.* **166** 49–55
Wardman P 2009 The importance of radiation chemistry to radiation and free radical biology *Br. J. Radiol.* **82** 89–104
Watts M E, Maughan R L and Michael B D 1978 Fast kinetics of the oxygen effect in irradiated mammalian cells *Int. J. Radiat. Biol.* **33** 195–9
Wenzl T and Wilkens J J 2011 Modelling of the oxygen enhancement ratio for ion beam radiation therapy *Phys. Med. Biol.* **56** 3251–68
Weyrather W K, Ritter S, Scholz M and Kraft G 1999 RBE for carbon track-segment irradiation in cell lines of differing repair capacity *Int. J. Radiat. Biol.* **75** 1357–64
Wilson P, Jones B, Yokoi T, Hill M and Vojnovic B 2012 Revisiting the ultra-high dose rate effect: implications for charged particle radiotherapy using protons and light ions *Br. J. Radiol. Br. J. Radiol.* **85** e933–9